Original Research Article

CdO nanostructures: synthesis, characterization, and photocatalytic degradation of malachite green dye in aqueous media

Abstract

Cadmium oxide (CdO) nanoparticles were prepared by using co-precipitation method and applied on photodegradation of malachite green (MG) dye in an aqueous solution. The as-prepared CdO formation of crystalline CdO nanoparticles with cubic structure while the FESEM image validated the preparation of disc-like spherical irregular shape nanostructures agglomerated with the size of 10-30 nm. The as- prepared CdO nanoparticles exhibited 98% photodegradation efficiency against the MG dye in 165 min of visible light irradiation at 0.05 g of dose. The experimental data has followed the pseudo-first-order kinetic model, and the rate constant value obtained is 0.002 min^{-1}. Thus, the synthesized CdO nanoparticles degraded MG dye effectively and may be used for environmental remediation purposes..

Keywords: CdO nanoparticles, MG dye, photodegradation efficiency, environmental remediation

1- INTRODUCTION

Cadmium oxide (CdO) is among of the semiconductors with an n-type II–IV and its direct band gap of 2.5 eV and an indirect band gap of 1.98 eV [1], thus it has wide usage such as solar cells, photo transistors, photo diodes, transparent electrodes and gas sensors [2]. The unique combination of high electrical conductivity, high carrier concentration and high transparency in the visible range of electromagnetic spectrum has prompted its optoelectronic applications [3]. Due to high reflectance in the infrared region, together with high transparency in the visible region, it is also used as heat mirrors. For these applications, particle size, porosity and specific surface area are of major importance. So far, a number of CdO nanostructures can be synthesized in different

morphologies shape such as nanowires [2,4,5], nanotubes [6], nanofibers [7], nanorods [8], nanoclusters [9], nanocubes [10], nanobelts [11], and nanoparticles [12] by different methods like hydrothermal method [13], template assisted method [14], solvothermal methods [15], chemical co-precipitation method [16], vapor phase transport [4], thermal evaporation [6], and sonochemical method [12].

On the other hand, water pollution one of the most serious environmental issues worldwide which has recently received a considerable attention. Enormous industries discharge their effluents, including toxic dyes (like malachalite green dye), into the aquatic environment without pretreatment such as plastic, paper, textile, and other industries [13, 14]. These contaminants have negative impacts on living systems and the environment and they are harmful. Among these negative impacts are ulcers, vomiting, irritation, methemoglobinemia, chemical burns, chest pain, respiratory issues, dyspnea, etc. [15–17]. Besides, dyes can cause several severe issues such as preventing the penetration of the sunlight into the aquatic environment, carcinogenicity, and toxicity [18]. Therefore, removing dyes from wastewater is a critical demand for keeping our environment safe; various research groups have devoted their effort to de-contaminating polluted wastewaters before their disposal. In this light, several physical, chemical, and biological methods such as membrane separation, electrochemical oxidation, coagulation, biological treatment, biodegradation, photocatalysis, adsorption, and ozonation have been reported [19–28]. The photocatalytic degradation process using nanomaterials has preferred because of its efficiency among these techniques owing to its simplicity, long-term applicability, and cost [29].

Therefore, based on the presented approach, we here in have developed a facile, one-pot, co-precipitation synthesis of cadmium oxide. XRD, FE-SEM, EDX, FT-IR and TEM techniques were used to characterize the as-prepared CdO nanoparticles. The photocatalytic degradation of malachite green (MG) dye using the as-prepared CdO nanoparticles was also investigated.

2. Experimental

2.1. Materials and reagents

Cadmium acetate dihydrate ($Cd(CH_3.COO)_2.2H_2O$) purchased from Loba Chime Company at Mumbai 40005 India, sodium hydroxide pellets (NaOH) and polyethylene glycol 6000 purchased from Fine Chem Company at Mumbai 30 India., distilled (Dist.) water, and the model molecule

malachite green (MG) dye ($C_{23}H_{25}ClN_4$, Scheme 1; (617 nm, 364.911 g/mol chloride)) were purchased from Sigma Aldrich Company. All materials and reagents used in the present work were of analytical grade and used as received without further purification.

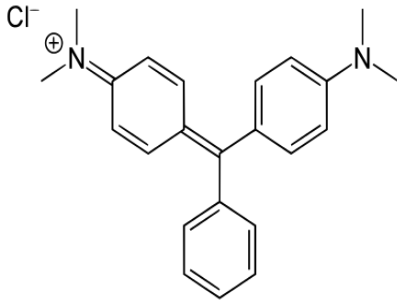

Scheme 1. Chemical molecular structure of MG model molecule.

2.2. Synthesis of CdO nanoparticles

CdO nanoparticles were prepared by using the coprecipitation method. In a typical synthesis, around 2.8 g of NaOH and 10ml of polyethylene glycol 6000 were dissolved into 50 mL dist. water and warmed with stirring (~200 rpm). Then, 1.33 g of $Cd(CH_3.COO)_2.2H_2O$ was added into 50 mL dist. water. Afterward, the solution of NaOH and polyethylene glycol 6000 was added drop by drop to the $Cd(CH_3.COO)_2.2H_2O$ solution. The final solution was stirred (~200 rpm) for 30 min. The product precipitate (CdO) was collected by centrifugation and then washed and dried after calcination at 400 ˚C for 1h.

2.3. Characterization

The morphology of the as-prepared CdO nanoparticles was investigated by scanning electron microscope (SEM, MIRA III XMU, TESCAN) equipped with an energy-dispersive X-ray spectrometer (EDS spectrometer). The particle size distributions in this technique appeared by image analysis.

The phase composition and crystallinity of the synthesized CdO nanoparticles was studied by using an X-ray powder diffractometer (XRD, Bruker Co. D8 Advanced) with Cu Ka radiation source (l ¼ 1.5406 A), with a generator voltage of 40 kV and 40 mA generator current (Central Metallurgical R&D Institute Cairo, Egypt). The XRD patterns were obtained from 4 to 80 (2θ) with a scanning step of (0.1). Fourier transform infrared (FT-IR) spectra were obtained using (Thermo Fisher, Nicolet IS10) spectrometer. The FT-IR spectra of the synthesized samples were

recorded at room temperature in the range from 4000 to 400 cm^{-1} to characterize the bond formation and functional groups of the samples under investigation.

The textural properties of the prepared CdO nanoparticles were investigated by high resolution transmission electron microscopy (HR-TEM) analysis and selected area electron diffraction (SAED) patterns. The HR-TEM as well as the corresponding SAED were performed by a (JEOL, JEM-2100) electron microscope equipped with a high-resolution gun, operated at an acceleration voltage of 200 kV.

The photocatalytic investigation was done by measuring the UV–Vis spectra of the MG dye solutions using a UV–Vis spectrophotometer (Jasco, model v670). The UV–Vis diffuse reflectance spectra of prepared products were carried out in the range of 400 – 800 nm. The UV-Vis spectroscopy was connected to an integral sphere (Jasco, Model ISN-723; Benha University, Egypt).

2.4. Photocatalytic studies

The photocatalytic activity of the CdO nanoparticles sample was evaluated through the degradation of MG dye using an in-house made reactor. This investigation was carried out by visible irradiation of a beaker containing the dye solution by using visible lamps (Philips at 365 nm 4 × 20 W). The source of the visible light was horizontally fixed at a 30 cm distance above the surface of the solution. In a typical photocatalytic experiment; the synthesized nanocatalyst quantity of (0.008, 0.01, 0.02, and 0.05 g) was dispersed in 50 mL of prepared MG dye solution with an initial concentration of 40 ppm. Then 0.05 g of the prepared nanocatalyst with different initial dye concentrations (40, 70, 60, and 70 ppm). Also, different pH solutions (4.6, 7.0, and 9.1) were investigated. The suspension was magnetically stirred in dark for 0.5 h to attain an adsorption-desorption equilibrium. Thereafter, the reaction mixture was stirred under visible illumination. At specific periods, aliquots were withdrawn out of the beaker, and the nanocatalyst suspension was separated by centrifugation. The concentration of the supernatant was evaluated using a Jasco UV–Vis spectrophotometer (Jasco, model v670). The kinetics of the dye photocatalytic degradation were also examined. The degradation efficiency percentage of the prepared catalyst is determined using the following equation (Eq. (1)):

$$\%\ \text{Degradation efficiency} = \left(\frac{C_0 - C_t}{C_0}\right) \times 100\% \qquad (1)$$

where C_0 (ppm) is the initial concentration of MG dye solution at zero time (i.e., before visible illumination) and C_t (ppm) is the remaining concentration of the MG dye after irradiation for time *t*.

The kinetics of the photocatalytic degradation of organic dyes normally follows the pseudo-first-order kinetics model of Langmuir– Hinshelwood mechanism. The kinetics of the photocatalytic degradation of MG dye is studied using pseudo-first-order kinetic Equation 2.

$$\ln\left(\frac{C_t}{C_0}\right) = -kt \qquad (2)$$

where C_0 and C_t are the initial concentration and concentration at t time of light illumination, k (min^{-1}) is the rate constant and time (t).

3. Results and discussion

3.1 Synthesis and characterization of CdO nanostructures

CdO nanoparticles were prepared using a facile co-precipitation method. This was performed by treatment of inexpensive materials (Section 2.1) for a relatively short time as mentioned earlier (Section 2.2). It is worth mentioning that the morphology and size generated which will be detailed later in our discussion. The products were characterized using XRD, FT-IR, FE-SEM, EDS, and TEM techniques.

3.1.1. XRD investigation

CdO nanoparticles can be investigate as in Fig. 2. shows the distinctive Bragg diffraction peaks of CdO nanoparticles as well indexed at (2θ) values of 33.02 (111), 38.31 (200), 55.30 (220), 65.93 (311), and 69.43 (222). These peaks correspond to database reference pattern JCPDS card no. 075-0592 with a cubic structure of CdO, space group of Fm-3m (225), and lattice parameters of a=b=c=4.6948 Å and Alpha= Beta= Gama=90° . The average crystalline sizes of the prepared CdO nanoparticles were estimated by using the Debye–Scherer formula (Eq. (3)) [30].So, it was observed that the average crystallite size of the CdO was 16.50 nm.

$$D = 0.9\lambda / \beta \cos\theta_B \qquad (3)$$

where, (2) θ_B is the Bragg diffraction angle, λ is the X-ray wavelength, and β is the XRD pattern peaks full width at half maximum (FWHM).

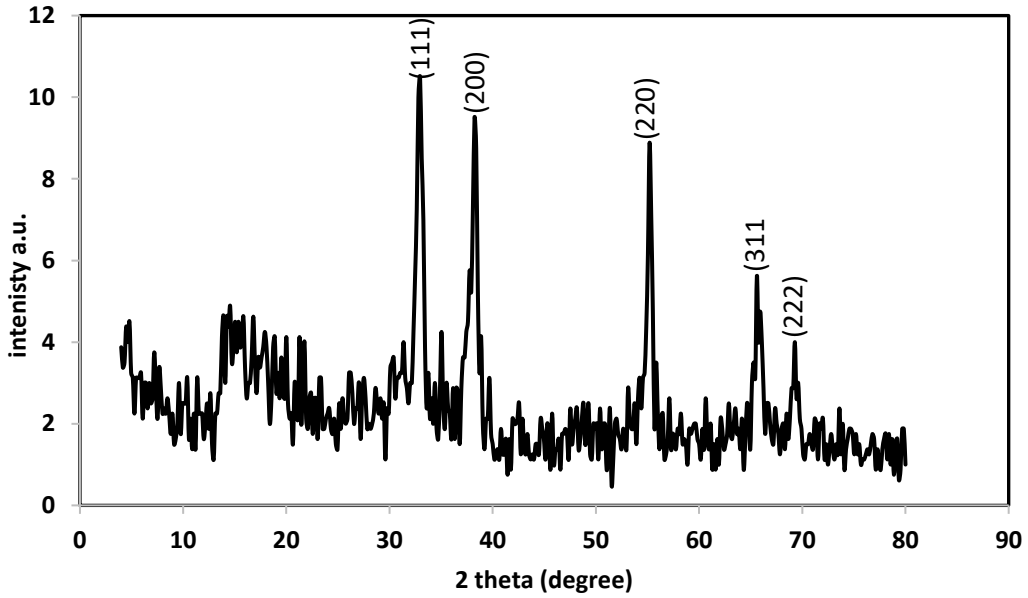

Figure 1. XRD pattern of CdO nanoparticles.

3.1.2 FT-IR study of CdO nanoparticles

The IR spectrum of the prepared CdO nanoparticles is shown in Fig. 2. The prepared CdO shows IR band at 1575 cm^{-1} is associated with symmetric stretching mode of C=O [31]. The band positioned at 1400 cm^{-1} is attributed to the –CH3 stretching bonds that might appear in cadmium acetate [32]. The IR bands shown in Fig. 2 are in the region of 1308 cm^{-1} correspond to CdO and band at 1000 cm^{-1} is assigned to C–O stretching vibrations of adsorbed CO_2. The characteristic bands in the range of 400-800 cm–1 correspond to Cd–O mode [33].

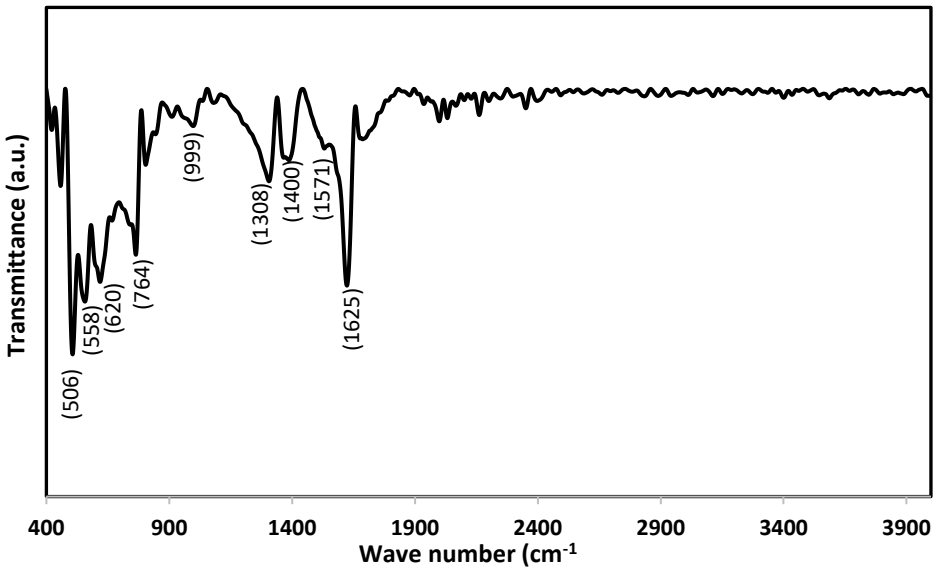

Figure 2. FT-IR spectra of prepared CdO nanoparticles

3.1.3 SEM and EDX studies of CdO nanoparticles

According to the SEM images shown in Figure 3 (a and b), the in-house prepared CdO nanoparticles appear to have primarily spherical agglomerated forms at the higher resolution and a mixture of agglomerated spherical and irregular shapes at the lower resolution. The uneven forms visible at lower resolutions imply some degree of coalescence or agglomeration, which may be caused by insufficient dispersion during synthesis controlling the particle development. The spherical shape shown at the greater resolution is in line with the usual morphology seen for colloidally produced CdO nanoparticles. Additionally, Cd and O make up most of the nanoparticles, according to the EDX results (Figure 3 c), with a weight percentage of 88.83% for Cd and 11.17% for O. The creation of CdO nanoparticles is confirmed by the high atomic percentage of Cd (53.1%) and the presence of O. The reduced weight percentage of O may be explained by the development of surface flaws or vacancies, which may affect the optical and electrical characteristics of the nanoparticles. All in all, the SEM and EDX examination indicates that the in-house prepared CdO nanoparticles exhibit an assortment of aggregated spherical and irregular forms, with primarily spherical shapes being found at greater resolution. CdO dominates the nanoparticles, although there are also a few surface vacancies or flaws.

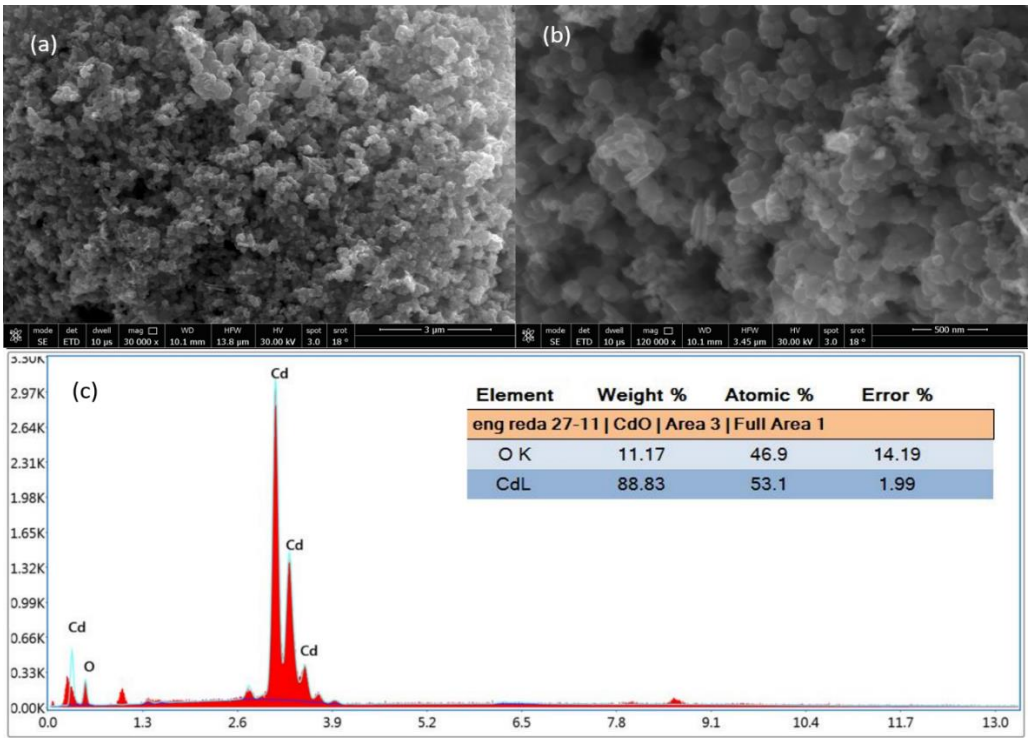

Figure 3. (a) and (b) FE-SEM images, and (c) EDX image of CdO nanoparticles.

3.1.4 TEM and SAED studies of CdO nanoparticles

For better understanding of the structural and morphological characteristics of the as-product CdO nanoparticles, has been explained by high-resolution transmission electron microscopy (HR-TEM), as shown in Fig. 4(a, b). Fig. 4(a, b) revealed that the product CdO is composed of dispersed polycrystalline coagulated particles with diffraction rang and one phase bond with an average diameter of 16.50 nm which is compatible with the crystallite size calculated from the XRD studies[34-36]. However, on inspection of the micrographs (c of Fig.4) it can be seen ~~that~~ the products with irregular agglomerate shape.

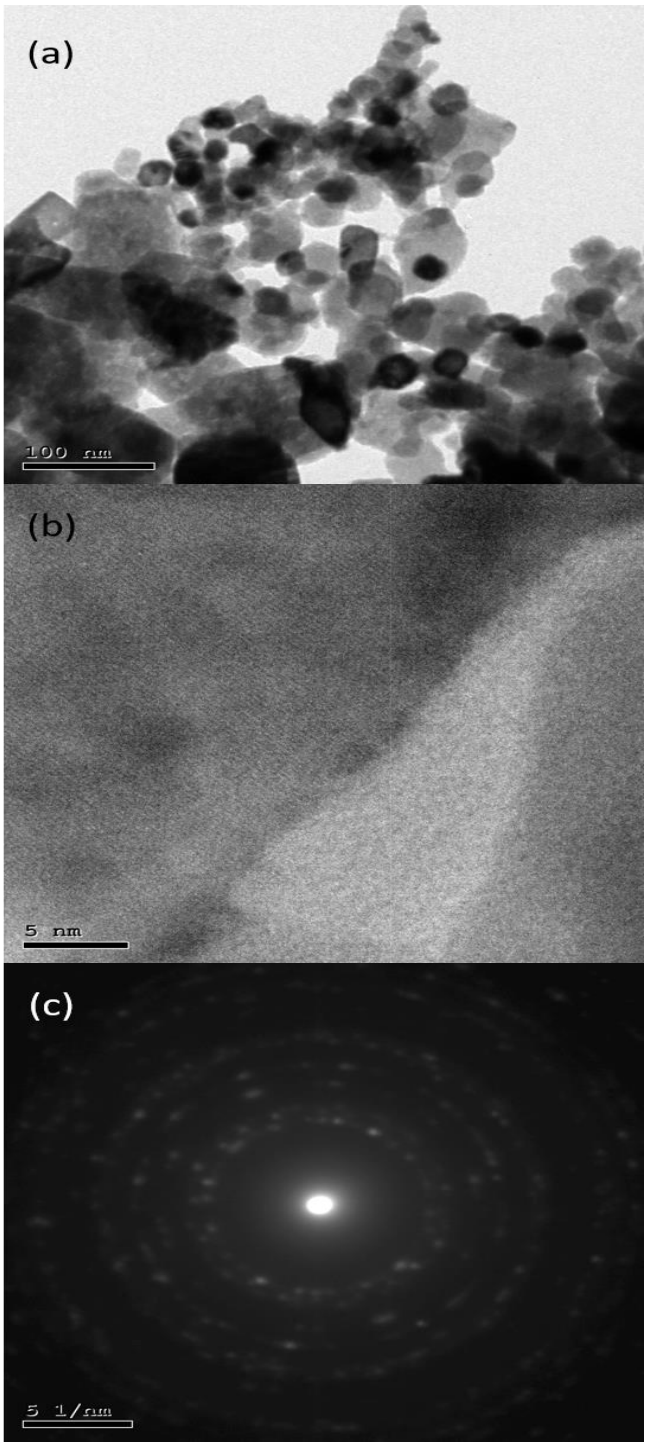

Fig .4 (a,b) HR-TEM images of CdO product (C) SAED patterns sample.

3.2. Photocatalytic activity and kinetic study of the prepared nanoparticles CdO

3.2.1. Effect of nanoparticles' dose

The photocatalytic activity of the prepared CdO nanoparticles were evaluated by photodegrading the model molecule (MG dye) under visible irradiation. The results show that the MG dye concentration decreases by increasing the irradiation time, in the presence of the synthesized nanoparticles. In which the absence of the photocatalyst, the photolysis of MG dye under the visible irradiation was negligible. Moreover, the results of photocatalytic degradation efficiency are shown in Fig. 5 (a). It can be also seen that the MG dye undergoes a negligible photo-degradation percentage (< 1%) in the absence of CdO nanoparticles. The influence of CdO photocatalyst dose (0.008, 0.01, 0.02, and 0.05 g) on the dye degradation efficiency was implemented, and the results are shown in Fig. (5 (a)). The results revealed that the photocatalytic degradation efficiency reached ca. 81 %, 83 %, 95 %, and 98 %, as shown in Fig (5(b)) for the applied catalyst doses, respectively, after visible irradiation for 165 min. This direct proportionality between the catalyst dose (0.008 − 0.05 g) and the photocatalytic degradation efficiency is probably returning to increasing the catalyst an irradiation time 0. The results exhibited that in the presence of the CdO surface area and the corresponding active sites, concentration of the MG dye decrease by increasing the irradiation time [37].

Furthermore, kinetics of photocatalytic degradation of MG dye under the visible irradiation were quantitatively explored by employing the pseudo-first-order kinetic equation (Eq. (3)). As presented in Fig. 5(c) for CdO dose. The kinetic results exhibited that the apparent degradation rate constants over CdO doses: 0.008, 0.010, 0.020, and 0.050 g, were 0.01008, 0.01065, 0.01815, and 0.02328 min^{-1}, respectively.

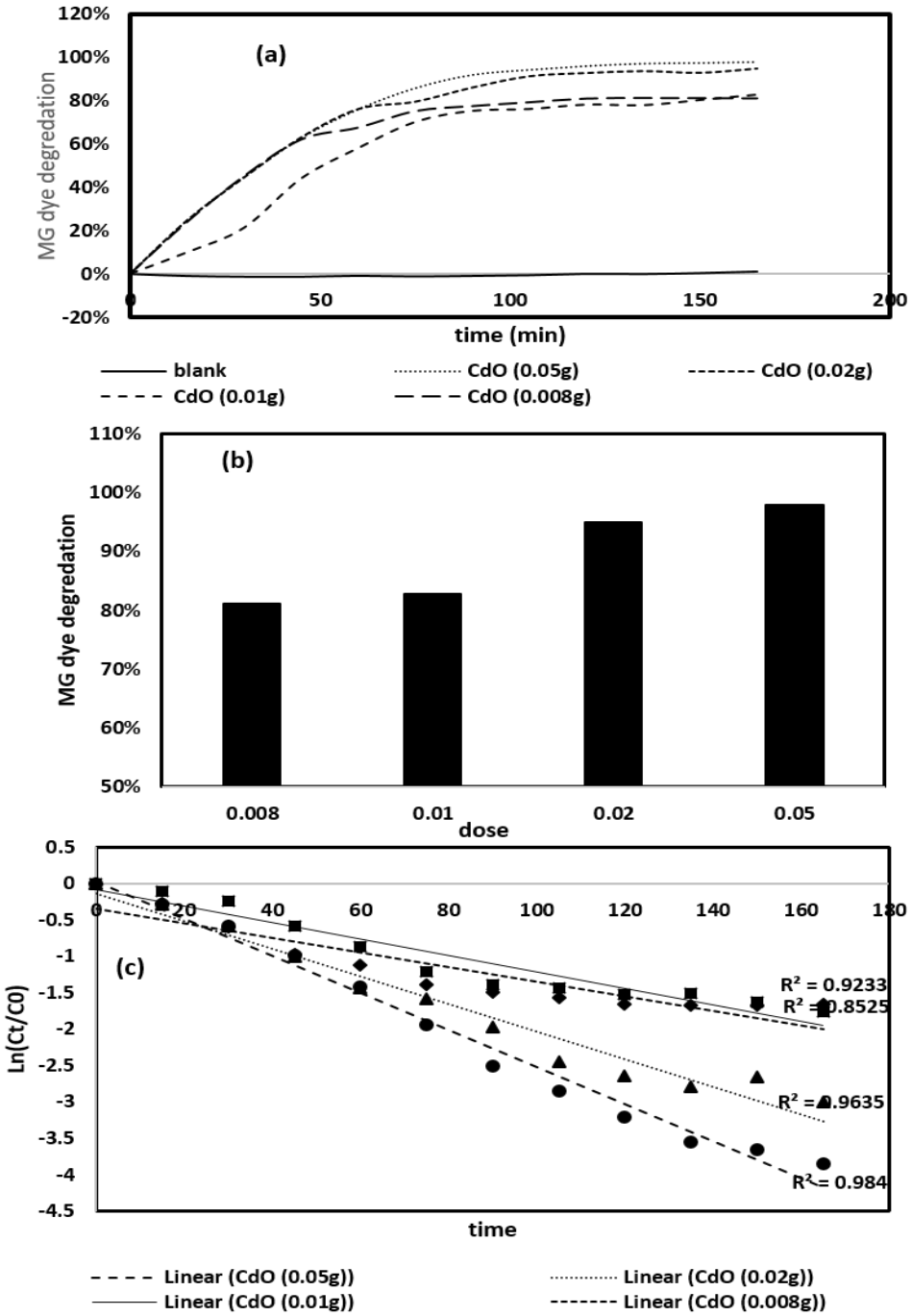

Figure 5. (a) Photocatalytic degradation efficiency (b) Degradation efficiency and (c) Degradation kinetic of dose (0.008, 0.01, 0.02, and 0.05 g) CdO with dye under visible light illumination.

3.2.2 Effect of MG dye initial concentration of MG

The influence of CdO nanoparticles dose (0.050 g) on different MG dye initial concentrations (70, 60, 50, and 40 ppm) was investigated. Thus, the results of dye degradation efficiency are shown in Fig. 6 (a). The results revealed that the photocatalytic degradation efficiency reached. 96 %, 97 %, 97 %, and 98 % (Fig 6 (a, b)) for the applied catalyst doses with different dye concentration, respectively, after visible irradiation for 165 min. that show inverse proportionality between the dye concentration and the photocatalytic degradation efficiency. The results exhibited that in the presence of the CdO surface area and the corresponding active sites, concentration of the MG dye decrease by increasing the irradiation time. And photodegradation increase with decrease dye concentration.

The apparent kinetic rate constants for the applied catalyst doses with different dye concentration (70, 60, 50, and 40 ppm,) were estimated by plotting Ln (Ct/C0) against time, as presented in Fig. 6(c) for CdO dose. The kinetic results exhibited that the apparent degradation rate constants over CdO dose were 0.02024, 0.02228, 0.02219, and 0.02328 min^{-1}, respectively.

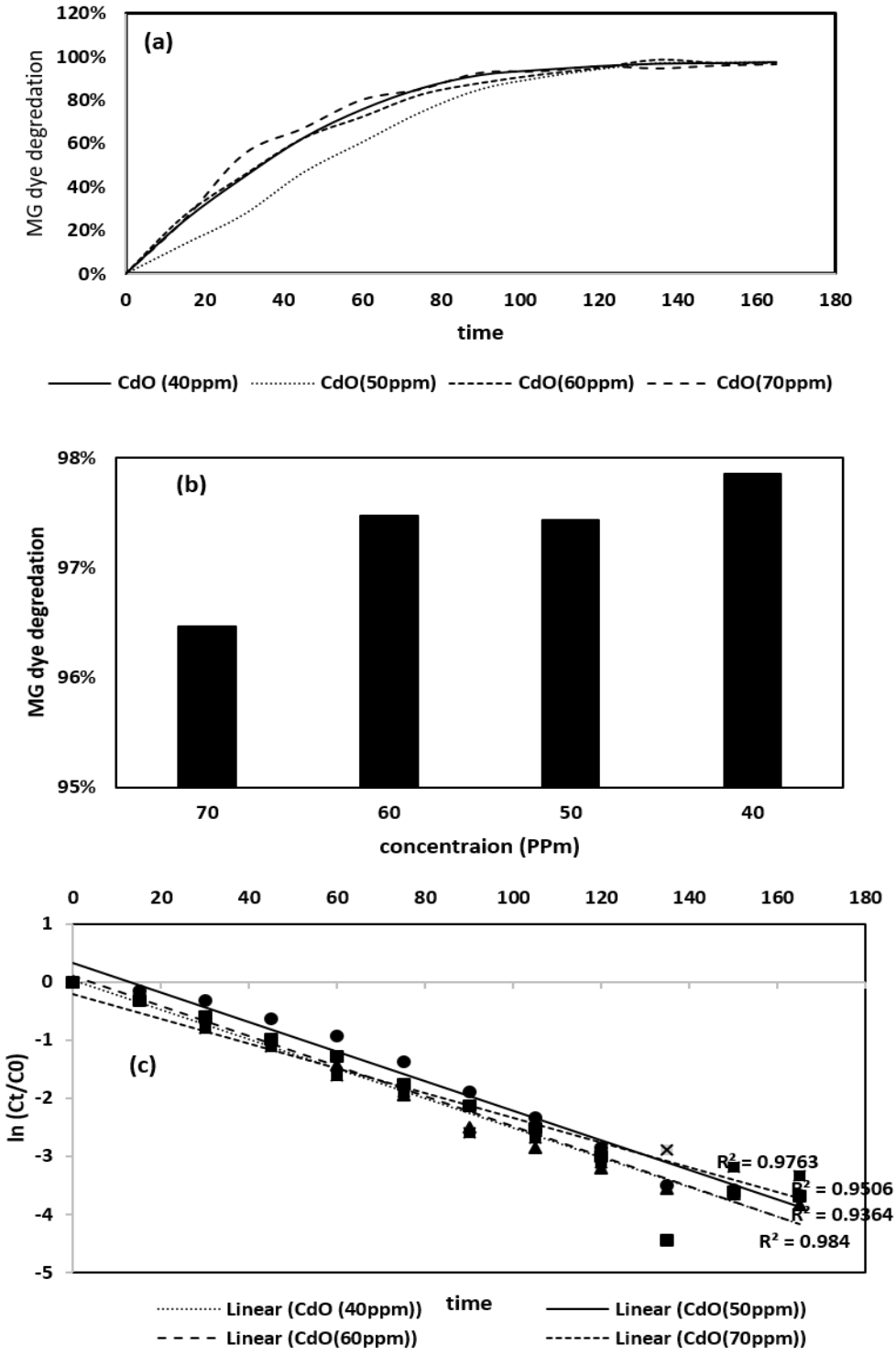

Figure 6. (a) Photocatalytic degradation efficiency (b) Degradation efficiency and (c) Degradation kinetic of CdO dose with various MG dye concentration: 70, 60, 50, and 40 ppm, under visible light illumination

3.2.3 Effect of pH of MG dye

The influence of CdO nanoparticles dose (0.050 g) with initial concentrations (40 ppm) on different PH MG dye (4.6, 7, and 9.1) was investigated. Thus, the results of dye degradation efficiency are shown in Fig. 7 (a). The results revealed that the photocatalytic degradation efficiency reached ca. 97 %, 98 %, and 100 % (Fig 7 (a, b)) for the applied catalyst doses with different dye PH, respectively, after visible irradiation for 165 min. that show inverse proportionality between the dye concentration and the photocatalytic degradation efficiency. The results exhibited that in the presence of the CdO surface area and the corresponding active sites, concentration of the MG dye decrease by increasing the irradiation time. And at acidic solution give smallest degradation efficiency.

The apparent kinetic rate constants for the applied catalyst doses with different dye concentration (4.6, 7, and 9.1) were estimated by plotting Ln (Ct/C0) against time, as presented in Fig. 7(c) for CdO dose. The kinetic results exhibited that the apparent degradation rate constants over CdO dose were 0.02072, 0.02328, and 0.03269 min^{-1}, respectively.

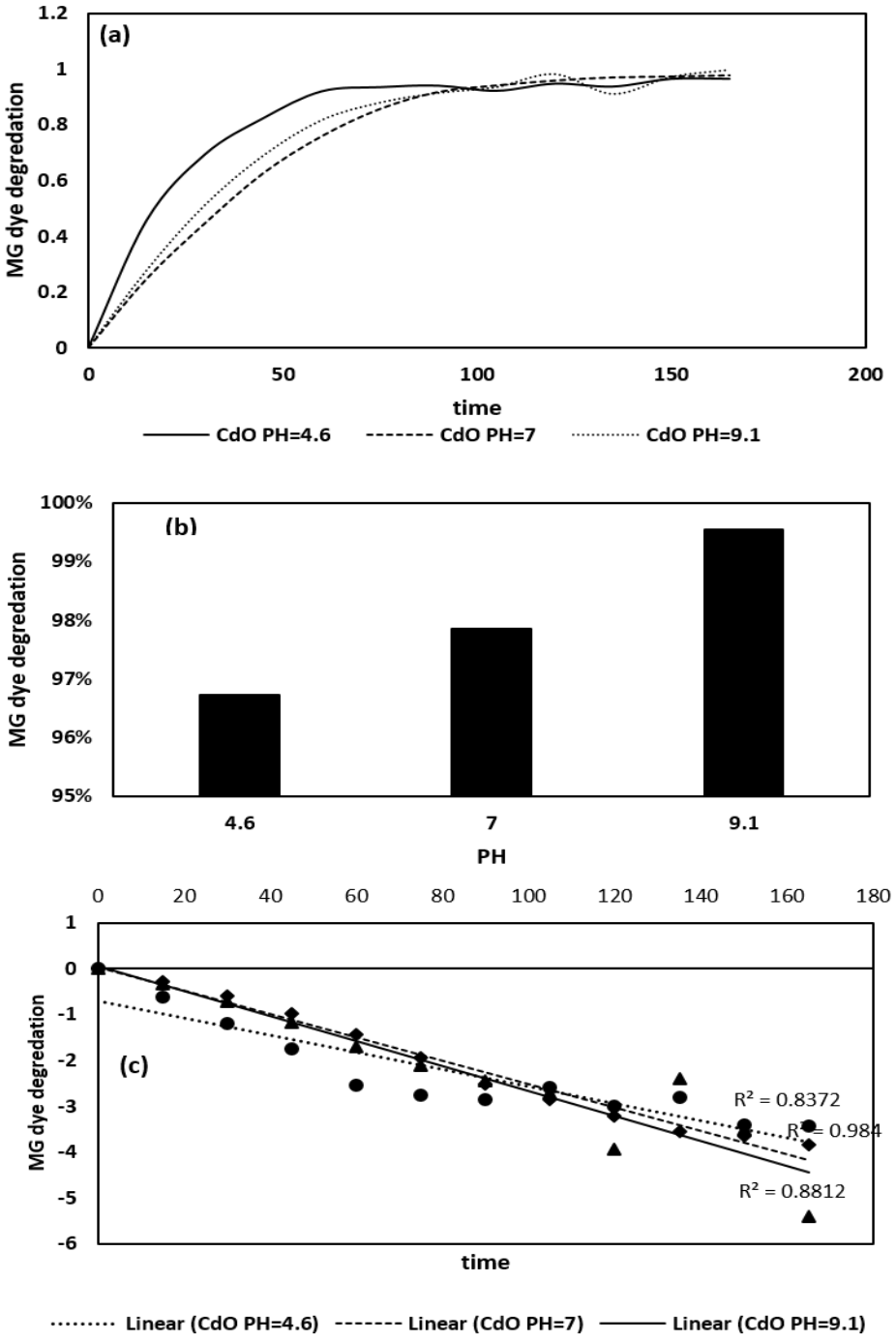

Figure 7. (a) Photocatalytic degradation efficiency (b) Degradation efficiency and (c) Degradation kinetic of CdO dose with various MG dye PH: 4.6, 7, and 9.1 under visible light illumination.

3.2.4 Photodegradation mechanism of CdO nanoparticles

The absorption of visible light photons (hυ) produce holes and electrons in the valence band (VB). The photo generated electrons get transferred from the VB to the conduction band (CB), whereas the holes stay in the VB. The photo generated holes and electrons act as oxidizing and reducing agents, respectively. The holes and electrons transfer to the surface of the catalyst from VB and CB and get trapped by water molecules and dissolved oxygen molecules, respectively, and consequently produce hydroxyl free radical (• OH) and superoxide radical anion (• O_2). Produced highly active free radical species react with the MG dye molecules and degrade them into intermediates, which are finally mineralized into non-hazardous inorganic CO_2 and H_2O molecules. The proposed possible photodegradation mechanism of MG for CdO catalyst is represented in Equations as in Fig 8.

$$CdO + h\upsilon \longrightarrow CdO\ (h^+ + e^-)$$

$$e^- + O_2 \longrightarrow O_2^{\bullet -}$$

$$O_2^{\bullet -} + 2H2O + e^- \longrightarrow 2HO^{\bullet} + 2HO^-$$

$$h^+ + H_2O \longrightarrow HO^{\bullet} + H^+$$

$$h^+ + HO^- \longrightarrow HO^{\bullet}$$

$$HO^{\bullet}/O_2^{\bullet -} + \text{MG dye} \longrightarrow \text{Intermediates}$$

$$\longrightarrow CO_2 + H_2O + \text{other products}$$

Figure 8 The possible photodegradation mechanism of MG for CdO catalyst is represented in Equations

4. Conclusions

In conclusion, cadmium oxide nanoparticles were successfully synthesized using co-precipitation method. Cadmium oxide have a significant influence on the purity, morphology, and crystallite size of the synthesized CdO nanostructure products. The nanoparticles prepared using for the photocatalytic degradation of Malachalite green (MG) dye from aqueous solutions. The removal percentage of (MG) dye reached ca. 98% in 165 min through the photocatalytic degradation over CdO nanoparticles under visible irradiation. In addition, the obtained data indicated the applicability of the as-prepared photocatalyst for the efficient removal of (MG) dye from aqueous solutions owing to its recyclability and stability. Accordingly, the as-prepared CdO nanoparticles can be proposed as a promising photocatalyst for the removal of (MG) dye from aqueous media.

References

[1] M. Ortega, G. Santana, A. Morales-Acevedo, Solid State Electron. 44 (2000) 1765.

[2] Q. Chang, C. Chang, X. Zhang, H. Ye, G. Shi, W. Zhang, Y. Wang, X. Xin, Y. Song, Opt. Commun. 274 (2007) 20.

[3] T.P. Gujar, V.R. Shinde, W.Y. Kim, K.D. Jung, C.D. Lokhande, O. Joo, Appl. Surf. Sci. 254 (2008) 3813.

[4] Tz Kuo, M.H. Huang, J. Phys. Chem. B 110 (2006) 13717.

[5] X.S. Peng, X.F. Wang, Y.W. Wang, C.Z. Wang, G.W. Meng, L.D. Zhang, J. Phys. D Appl. Phys. 35 (2002)1.

[6] H.B. Lu, L. Liao, H. Li, Y. Tian, D.F. Wang, J.C. Li, Q. Fu, B.P. Zhu, Y. Wu, Mater. Lett. 62 (2008) 3928.

[7] A.M. Bazargan, S.M.A. Fateminia, M.E. Ganji, M.A. Bahrevar, Chem. Eng. J. 155 (2009) 523.

[8] R.R. Salunkhe, D.S. Dhawale, U.M. Patil, C.D. Lokhande, Sens. Actuators B 136 (2009) 39.

[9] B.S. Zou, V.V. Volkov, Chem. Mater. 11 (1999) 3037.

[10] J.H. Kim, Y.C. Hong, H.S. Uhm, Jap. J. Appl. Phy. 46 (2007) 4351.

[11] Z.W. Pan, Z.R. Dai, Z.L. Wang, Science 291 (2001) 1947.

[12] A. Askarinejad, A. Morsali, Mater. Lett. 62 (2008) 478.

[13] M.Y. Nassar, S. Abdallah, Facile controllable hydrothermal route for a porous CoMn2O4 nanostructure: synthesis, characterization, and textile dye removal from aqueous media, RSC Adv. 6 (2016) 84050–84067.

[14] M.Y. Nassar, M. Khatab, Cobalt ferrite nanoparticles via a template-free hydrothermal route as an efficient nano-adsorbent for potential textile dye removal, RSC Adv. 6 (2016) 79688–79705.

[15] N.F. Cardoso, R.B. Pinto, E.C. Lima, T. Calvete, C.V. Amavisca, B. Royer, M. L. Cunha, T.H.M. Fernandes, I.S. Pinto, Removal of remazol black B textile dye from aqueous solution by adsorption, Desalination 269 (2011) 92–103.

[16] B. Kayan, B. Gozmen, ¨ M. Demirel, A.M. Gizir, Degradation of acid red 97 dye in aqueous medium using wet oxidation and electro-Fenton techniques, J. Hazard. Mater. 177 (2010) 95–102.

[17] M. Kamaraj, N.R. Srinivasan, G. Assefa, A.T. Adugna, M. Kebede, Facile development of sunlit ZnO nanoparticles-activated carbon hybrid from pernicious weed as an operative nano-adsorbent for removal of methylene blue and chromium from aqueous solution: extended application in tannery industrial wastewater, Environ. Technol. Innov. 17 (2020), 100540.

[18] M.Y. Nassar, E.I. Ali, E.S. Zakaria, Tunable auto-combustion preparation of TiO2 nanostructures as efficient adsorbents for the removal of an anionic textile dye, RSC Adv. 7 (2017) 8034–8050.

[19] M.Y. Nassar, A.S. Amin, I.S. Ahmed, S. Abdallah, Sphere-like Mn2O3 nanoparticles: facile

hydrothermal synthesis and adsorption properties, J. Taiwan Inst. Chem. Eng. 64 (2016) 79–88.

[20] M.Y. Nassar, M.M. Moustafa, M.M. Taha, Hydrothermal tuning of the morphology and particle size of hydrozincite nanoparticles using different counterions to produce nanosized ZnO as an efficient adsorbent for textile dye removal, RSC Adv. 6 (2016) 42180–42195.

[21] M. Djenouhat, O. Hamdaoui, M. Chiha, M.H. Samar, Ultrasonication-assisted preparation of water-in-oil emulsions and application to the removal of cationic dyes from water by emulsion liquid membrane: part 2, Permeation and stripping, Separation and Purification Technology 63 (2008) 231–238.

[22] A.B. Fradj, S.B. Hamouda, H. Ouni, R. Lafi, L. Gzara, A. Hafiane, Removal of methylene blue from aqueous solutions by poly(acrylic acid) and poly(ammonium acrylate) assisted ultrafiltration, Sep. Purif. Technol. 133 (2014) 76–81.

[23] D. Robati, M. Rajabi, O. Moradi, F. Najafi, I. Tyagi, S. Agarwal, V.K. Gupta, Kinetics and thermodynamics of malachite green dye adsorption from aqueous solutions on graphene oxide and reduced graphene oxide, J. Mol. Liq. 214 (2016) 259–263.

[24] E. Pajootan, M. Arami, N.M. Mahmoodi, Binary system dye removal by electrocoagulation from synthetic and real colored wastewaters, J. Taiwan Inst. Chem. Eng. 43 (2012) 282–290.

[25] Q. Wu, W.-T. Li, W.-H. Yu, Y. Li, A.-M. Li, Removal of fluorescent dissolved organic matter in biologically treated textile wastewater by ozonation-biological aerated filter, J. Taiwan Inst. Chem. Eng. 59 (2016) 359–364.

[26] A. Mohammadzadeh, M. Ramezani, A.M. Ghaedi, Synthesis and characterization of Fe2O3–ZnO–ZnFe2O4/carbon nanocomposite and its application to removal of bromophenol blue dye using ultrasonic assisted method: optimization by response surface methodology and genetic algorithm, J. Taiwan Inst. Chem. Eng. 59 (2016) 275–284.

[28] S. Barathi, C. Karthik, I.A. Padikasan, Biodegradation of textile dye Reactive Blue 160 by Bacillus firmus (Bacillaceae: bacillales) and non-target toxicity screening of their degraded products, Toxicol. Rep. 7 (2020) 16–22.

[28] J.M.S. Oliveira, M.R. de Lima e Silva, C.G. Issa, J.J. Corbi, M.H.R.Z. Damianovic, E. Foresti, Intermittent aeration strategy for azo dye biodegradation: a suitable alternative to conventional biological treatments? J. Hazard. Mater. 385 (2020), 121558.

[29] H.-F. Zhai, A.-D. Li, J.-Z. Kong, X.-F. Li, J. Zhao, B.-L. Guo, J. Yin, Z.-S. Li, D. Wu, Preparation and visible-light photocatalytic properties of BiNbO4 and BiTaO4 by a citrate method, J. Solid State Chem. 202 (2013) 6–14.

[30] R. Jenkins and R. L. Snyder, Chemical Analysis: Introduction to X-ray Powder Diffractometry, John Wiley and Sons, Inc., New York, 1996.

[31] P. Bhadra, M.K. Mitra, G.C. Das, R. Dey, S. Mukherjee, Interaction of chitosan capped ZnO nanorodes with Escherichia coli, Mater. Sci. Eng. C 31 (5) (2011) 929e937.

[32] S. Zandi, P. Kameli, H. Salamati, H. Ahmadvand, M. Hakimi, Microstructure and optical properties of ZnO nanoparticles prepared by a simple method, Phys. B Con. Mater. 406 (17) (2011) 3215e3218.

[33] B. Malecka, A. Lacz, Thermal deposition of cadmium formate in inert and oxidative atmosphere, Thermochim. Acta 479 (1e2) (2008) 12e16.

[34] K.J.M. Bishop, C.E. Wilmer, S. Soh, B.A. Grzybowski, Small 5 (2009) 1600.

[35] J.J. Freedsman, L.J. Kennedy, R.T. Kumar, G. Sekaran, J.J. Vijaya, Mater. Res. Bull. 45 (2010) 1481.

[36] Y.C. Zhang, G.L. Wang, Mater. Lett. 62 (2008) 673.

[37] M. Usman, A. Ahmed, B. Yu, Q. Peng, Y. Shen, H. Cong, Photocatalytic potential of bio-engineered copper nanoparticles synthesized from Ficus carica extract for the degradation of toxic organic dye from waste water: growth mechanism and study of parameter affecting the degradation performance, Mater. Res. Bull. 120 (2019), 110583.